

Behavior of the Fermi-edge singularity in the photoluminescence spectra of a high-density two-dimensional electron gas

H. Kissel,* U. Zeimer, A. Maaßdorf, and M. Weyers

Ferdinand-Braun-Institut für Höchstfrequenztechnik, Albert-Einstein-Strasse 11, 12489 Berlin, Germany

R. Heitz and D. Bimberg

Institut für Festkörperphysik, Technische Universität Berlin, Hardenbergstrasse 36, 10623 Berlin, Germany

Yu. I. Mazur,† G. G. Tarasov,‡ Vas. P. Kunets, U. Müller, Z. Ya. Zhuchenko,‡ and W. T. Masselink
Institut für Physik, Humboldt-Universität zu Berlin, Invalidenstrasse 110, 10115 Berlin, Germany

(Received 14 March 2001; revised manuscript received 22 February 2002; published 12 June 2002)

Fundamentally different behavior of the Fermi-edge singularity (FES) in photoluminescence of heavily doped pseudomorphic modulation-doped $\text{Al}_x\text{Ga}_{1-x}\text{As}/\text{In}_y\text{Ga}_{1-y}\text{As}/\text{GaAs}$ heterostructures is observed. The noteworthy features are: (i) the FES enhancement from E_F of $n=1$ electronic subband is observed under condition of the $n=2$ subband population, (ii) the heavy-hole localization energy is directly observed in the FES development, (iii) the magnitude of the FES increases with increasing temperature at low temperatures, and (iv) the FES is a nonmonotonic function of the excitation density. A qualitative analysis is performed in terms of heavy-hole localization by potential fluctuations in the $\text{In}_y\text{Ga}_{1-y}\text{As}$ quantum well.

DOI: 10.1103/PhysRevB.65.235320

PACS number(s): 78.55.Cr, 71.27.+a, 73.40.Kp

I. INTRODUCTION

The Fermi-edge singularity (FES)¹⁻⁴ originates from the response of a degenerate two-dimensional electron gas (2DEG) to the photogeneration or annihilation of a positively charged hole and is one of the most widely studied manifestations of many-body effects observed in the optical spectra of semiconductor heterostructures. This interaction results in an enhanced oscillator strength for electrons near the Fermi surface recombining with photogenerated holes, an effect whose principle features are relatively well understood theoretically.⁵⁻⁷ The current theoretical picture of the Fermi-edge singularity contains the following components: (i) the self-consistent Born approximation and a rigid Fermi sea for excitonic corrections,^{8,9} (ii) the resonance between the Mahan excitons (rigid Fermi surface) of the occupied subband ($n=1$) and the exciton state originating from the empty subband ($n=2$),¹⁰ (iii) both the dynamical response of the Fermi sea and excitonic effects in the presence of a localized hole,¹¹ and (iv) the multiple electron-hole scattering and an appropriate screening within the Bethe-Salpeter equation^{1,12} and primarily describes the case of thermalized hole, low temperature, and low excitation density. As a result, these models describe the FES appearance in the photoluminescence (PL) of semiconductor systems with strong hole localization [the case of modulation-doped $\text{In}_y\text{Ga}_{1-y}\text{As}$ quantum well (QW)], and predict its rapid degradation under increased temperature and excitation density.

Several experimental results,¹³⁻¹⁷ however, are not fully understood within the existing theoretical framework. Brown *et al.*,¹⁵ for example, observed Fermi-edge enhancement of the PL even in $\text{GaAs}/\text{Al}_x\text{Ga}_{1-x}\text{As}$ multiple QW samples, involving both light and heavy holes; this effect is apparently unrelated to the hole localization or the proximity of a second electronic subband. A recent study of collective effects in optical spectra of GaAs QW's (Ref. 16) has also demon-

strated the FES appearance in PL excitation spectra in high-density 2DEG with delocalized holes if the electron mobility is high ($\mu \sim 10^5 - 10^6 \text{ cm}^2/\text{Vs}$). It was suggested that the role of hole localization in the screening properties of a high-density 2DEG (and therefore in the FES) has to be reexamined. Lastly, the results of Mélin and Laruelle^{18,19} refer to a more realistic many-body theory including disorder and multiple subbands. The extrinsic inter-subband scattering requires an accurate evaluation while analyzing FES in $\text{Al}_x\text{Ga}_{1-x}\text{As}$ QW's.¹⁹ Finally, PL investigations in pseudomorphic modulation-doped $\text{Al}_x\text{Ga}_{1-x}\text{As}/\text{In}_y\text{Ga}_{1-y}\text{As}/\text{GaAs}$ heterostructures²⁰ and in low-doped $\text{In}_y\text{Ga}_{1-y}\text{As}/\text{InP}$ heterostructures²¹ have convincingly shown that the carrier concentration and the excitation density strongly influence the FES development even in the presence of hole localization, again contrary to theoretical expectations.

In this paper we investigate the FES under conditions that are prohibited according to existing theoretical models and revise the understanding of which experimental conditions allow the FES. Specifically, we demonstrate the Fermi enhancement of the PL spectrum from the $n=1$ conduction subband, although the second subband is occupied; we directly measure the localization energy of the heavy hole in the FES recombination; and we show that the FES recombination intensity can *increase* with increasing temperature and excitation density. These results are presented as the basis for a reform of the current theoretical understanding; furthermore, a qualitative picture accounting for the finite mass of the valence hole in a realistic way, hole localization, and, more generally, the dynamic response of the Fermi sea is presented.

II. EXPERIMENTAL DETAILS

Pseudomorphic modulation-doped $\text{Al}_x\text{Ga}_{1-x}\text{As}/\text{In}_y\text{Ga}_{1-y}\text{As}/\text{GaAs}$ heterostructures with an $\text{In}_y\text{Ga}_{1-y}\text{As}$ QW

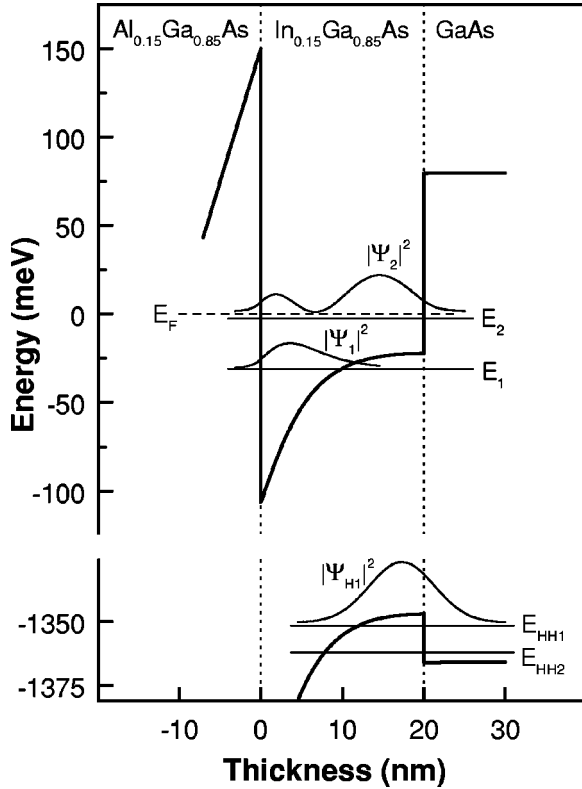


FIG. 1. Conduction- and valence-band profiles for sample 1 calculated using the coupled Schrödinger-Poisson equations. Squared envelope functions for electrons and holes in some of their subbands are also shown. Distance is measured from AlGaAs/InGaAs interface position.

containing more than one populated subband were prepared using gas-source molecular-beam epitaxy in order to investigate in detail the FES development influenced by the close proximity of the $n=2$ electronic subband. The typical epilayer sequence consists of a GaAs buffer layer ($d=300$ nm), an undoped $\text{In}_y\text{Ga}_{1-y}\text{As}$ strained QW (2DEG channel) with width d_W , an $\text{Al}_x\text{Ga}_{1-x}\text{As}$ undoped spacer ($x=0.2$, $d=7.5$ nm), an $\text{Al}_x\text{Ga}_{1-x}\text{As}$ heavily Si-doped supplier layer ($x=0.2$, $d=35$ nm, $N_D=2 \times 10^{18}$ cm^{-3}), and a Si-doped GaAs cap layer ($d=5$ nm, $N_D=2.5 \times 10^{18}$ cm^{-3}). Double-crystal x-ray diffraction and simulation of the rocking curves were used to control the samples' structural parameters and to ensure high structural quality. Reciprocal space maps at the $(\bar{2}\bar{2}4)$ reflection were used to verify that no strain relaxation by generation of misfit dislocations occurred, i.e., the investigated samples are fully pseudomorphic.

The PL was excited by the 514.5-nm line of a cw Ar^+ laser and focused to a spot size of 200 μm . The PL signal was dispersed through a 3/4-meter Czerny-Turner scanning spectrometer, with a spectral resolution better than 0.1 meV, and sensed using phase-sensitive detection with a thermoelectrically cooled photomultiplier tube [containing a GaAs(Cs) photocathode] or a liquid-nitrogen (LN_2)-cooled high-purity Ge detector. The samples were mounted in an Oxford Spectromag 4000 system that allows measurements

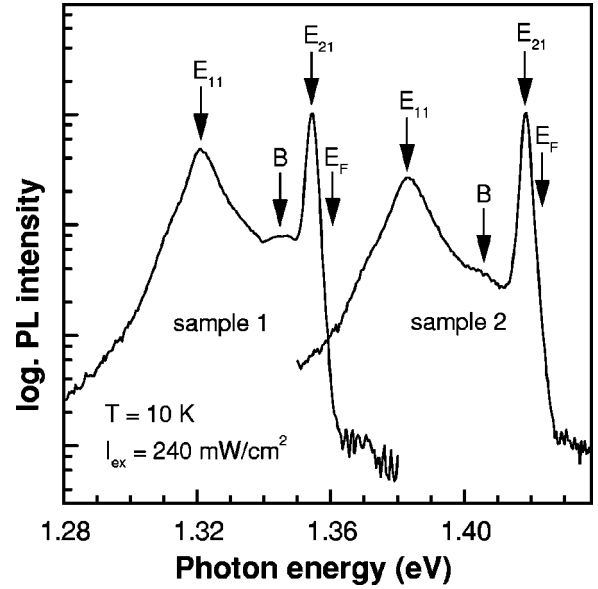


FIG. 2. PL spectra for sample 1 and sample 2. Arrows show the positions of the E_{11} and E_{21} transitions, the enhancement of feature B, and the Fermi energy E_F .

in magnetic fields up to 7 T and at temperatures from 1.7 to 300 K.

The PL excitation (PLE) were taken in a continuous-flow He cryostat with a tungsten lamp dispersed by a 0.27-m double-grating monochromator as a tunable light source and a 0.3-m double-grating monochromator with a LN_2 -cooled Ge photodiode for detection.

Two representative samples from a series are further described. Sample 1 has $y=0.15$, QW thickness $d_W=20$ nm, and the electron sheet density $n_s=1.21 \times 10^{12}$ cm^{-2} ; while sample 2 has $y=0.10$, $d_W=20$ nm, and $n_s=1.05 \times 10^{12}$ cm^{-2} . The electron density n_s is determined from Hall measurements down to 12 K.

III. RESULTS AND DISCUSSION

The electron subband structure for the $\text{In}_y\text{Ga}_{1-y}\text{As}$ QW, calculated from the self-consistent solution of coupled Schrödinger and Poisson equations is shown in Fig. 1 for sample 1. The $n=2$ subband is filled by 2DEG at the lowest temperature while $\Delta E \equiv E_F - E_2 = 3$ meV. Under a near-resonance condition between the $n=2$ subband and the Fermi level of the 2DEG one can expect the behavior described by Skolnick *et al.*²² for a similar situation: the FES should be controlled by the carrier density in the subband in which the excitonic enhancement occurs.

Our data show, however, fundamentally different behavior of the FES, strongly differing from that described in Refs. 20, 22 and 23. Figure 2 depicts the PL spectra of sample 1 and sample 2 taken at low temperatures ($T=10$ K). Besides the dominating features related to optical transitions between the E_1 and E_2 electronic subbands and $n=1$ heavy-hole subband (low-energy E_{11} and high-energy E_{21} PL bands, respectively) one sees a distinct feature (marked as feature B) in the spectral range between the PL peaks. This feature demon-

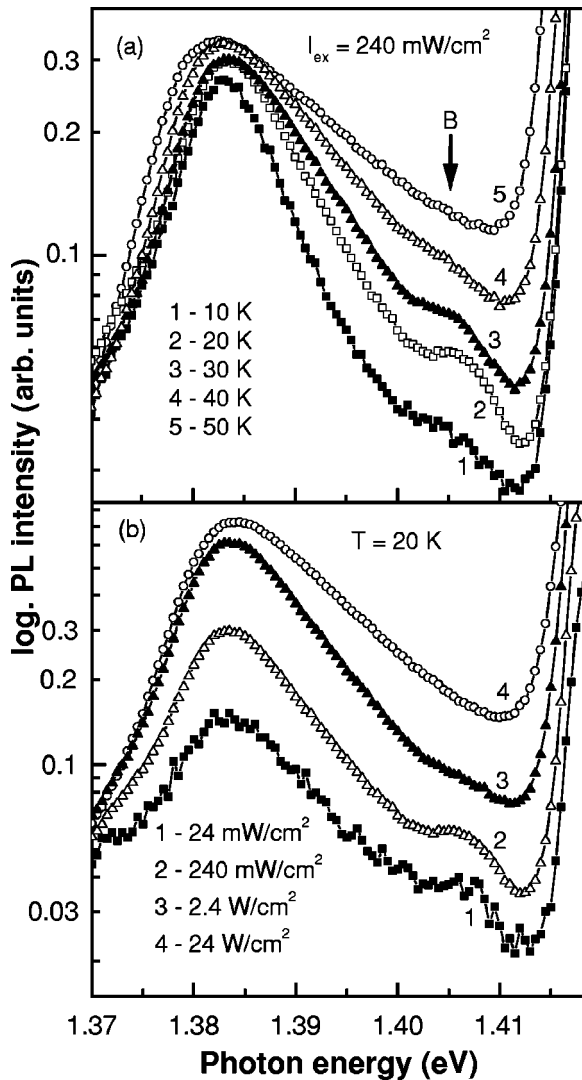


FIG. 3. Temperature (a) and excitation (b) dependent evolution of the PL spectra in sample 2. The position of feature B is marked by an arrow.

strates a characteristic temperature sensitivity. An increase in temperature of 10 K causes it to completely disappear apparently due to its low binding energy, the order of 1 meV typically for many-body effects.

Figure 3 shows the photoluminescence dependence on temperature (a) and on excitation density (b) for sample 2. Barely visible for $T < 10$ K and $I < 24$ mW/cm² (this case is not shown), the spectral feature B increases in magnitude as either the temperature or the excitation density is increased, emerging as a distinct peak separated by 10 meV from E_{21} transition (for $T = 10$ K and $I = 240$ mW/cm²) [see Fig. 3(a)]. Further increase in temperature beyond 20 K or excitation intensity beyond 240 mW/cm² results in a washing out of feature B. The nonmonotonic dependence of feature's B magnitude on T and I implies the existence of optimal temperature and intensity conditions for its observation.

A similar behavior is observed also in other samples of our series. Figure 4 shows the dependence of the PL spectrum on temperature (a) and excitation density (b) in sample

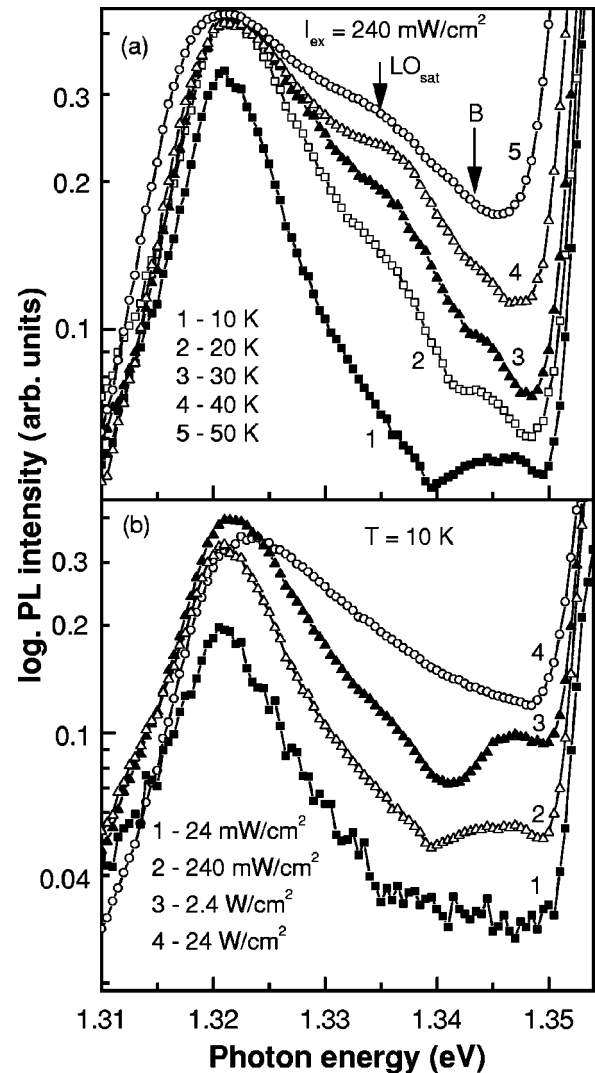


FIG. 4. Temperature (a) and excitation (b) dependent development of the PL in sample 1. Feature B and the LO satellite of optical transitions at the top of the Fermi sea are marked by arrows.

1. Indeed, feature B positioned at the red side of the E_{21} band reveals even more drastic (T, I) dependence, than that in the PL spectra of sample 2. In addition, another feature at the blue side of the E_{11} transition appears and steadily grows with increasing temperature. This broad shoulder is clearly observed even at $T > 50$ K while the high-energy feature B decays completely. The shoulder lies 36.5 meV [the longitudinal-optical (LO)-phonon energy for GaAs] below $E_g + E_F$ and is attributed to LO-phonon-assisted scattering of electrons at the top of the Fermi sea.

Before discussing the experimental data and their meaning, we first describe the analysis technique in some detail. Apparently, the Fano resonance mechanism controls the formation of optical FES in multi-subband systems, such as pseudomorphic modulation-doped $\text{Al}_x\text{Ga}_{1-x}\text{As}/\text{In}_y\text{Ga}_{1-y}\text{As}/\text{GaAs}$ (Refs. 24 and 25) and/or remotely doped $\text{Al}_x\text{Ga}_{1-x}\text{As}$ heterostructures.¹⁹ Under thermal activation above $E_g + E_F$ or excitation density elevation the PL from the empty $n = 2$ subband develops into a dominant

excitonlike feature E_{2x} of high oscillator strength and discrete character. The 2DEG PL (E_{11} transition) extends from transitions near the $n=1$ subband bottom ($k \cong 0$) up to transitions at $k=k_F$. According to the Fano resonance between a discrete excitonic state and the continuum of Fermi-sea excitations the PL profile is described analytically as^{19,26}

$$I(E) \propto f(E) \frac{A^2 + B(E)^2}{1 + B(E)^2}. \quad (1)$$

The experimental oscillator strength A^2 of the excitonic resonance relative to the continuum is quite sensitive to small geometrical fluctuations. $B = (E - E_{2x})/\Gamma$ with $\Gamma = \pi W^2 D$, W is the statistically averaged interaction matrix element, and D is the density of states for the $n=1$ conduction subband.

According to Eq. (1) two hybridized states, separated by a spectral dip (antiresonance) and caused by a destructive interference, interact resulting in the high-energy side asymmetry for the excitonic state and the enhanced oscillator strength for the continuum transitions.

Focusing on the temperature behavior of the observed experimental PL spectra, the thermal quenching of the blue-side spectral feature of E_{11} transition (seen in Figs. 3 and 4) could be interpreted as a disappearance of the relative PL minimum between $E_g + E_F$ and E_{2x} in Fano resonance with increasing temperature. From many-body theories, requiring an abrupt Fermi edge for the enhancement of multiple Coulomb scattering at E_F , a similar quenching is expected.

Using the Fano resonance mechanism to explain $\Delta = E_{2x} - E_g - E_F$ and temperature variations in the low-temperature PL spectra of $\text{Al}_x\text{Ga}_{1-x}\text{As}/\text{GaAs}$ heterostructures, Mélin and Laruelle¹⁹ excluded the enhancement of many-body processes due to hole localization. On the other hand, the alloy disorder contributes mainly to the intersubband coupling.

From the peculiarities of the thermal and excitation density behavior observed in our samples related to feature B , we conclude that the Fano resonance mechanism is not applicable here. Indeed, both temperature and excitation density elevation tend to destroy the resonance conditions. Therefore, the Fano resonance concept is hardly coherent with the increase of the observed PL feature strength. The existence of the E_{2x} exciton is also questionable for our systems with respect to the filling of the $n=2$ conduction subband. The PL spectra give clear evidence of such a band filling (see Figs. 3 and 4).

It should be noted that an additional peak has been also detected earlier in the PL spectra of pseudomorphic $\text{GaAs}/\text{In}_{0.2}\text{Ga}_{0.8}\text{As}/\text{Al}_{0.25}\text{Ga}_{0.75}\text{As}$ modulation-doped single QW's (Ref. 27) similar to our heterostructures. It was ascribed to the strong coupling between the $\text{In}_y\text{Ga}_{1-y}\text{As}$ QW and the potential well formed in the $\text{Al}_x\text{Ga}_{1-x}\text{As}$ barrier due to planar doping. This coupling produces hybrid states in the conduction band giving rise to additional transitions in the emission spectrum. One of these transitions between hybrid electronic state and heavy-hole state could be responsible for the extra PL peak observed below the E_{21} transitions. The strongly nonmonotonic temperature dependence of the peak strength, however, makes such an assignment somewhat

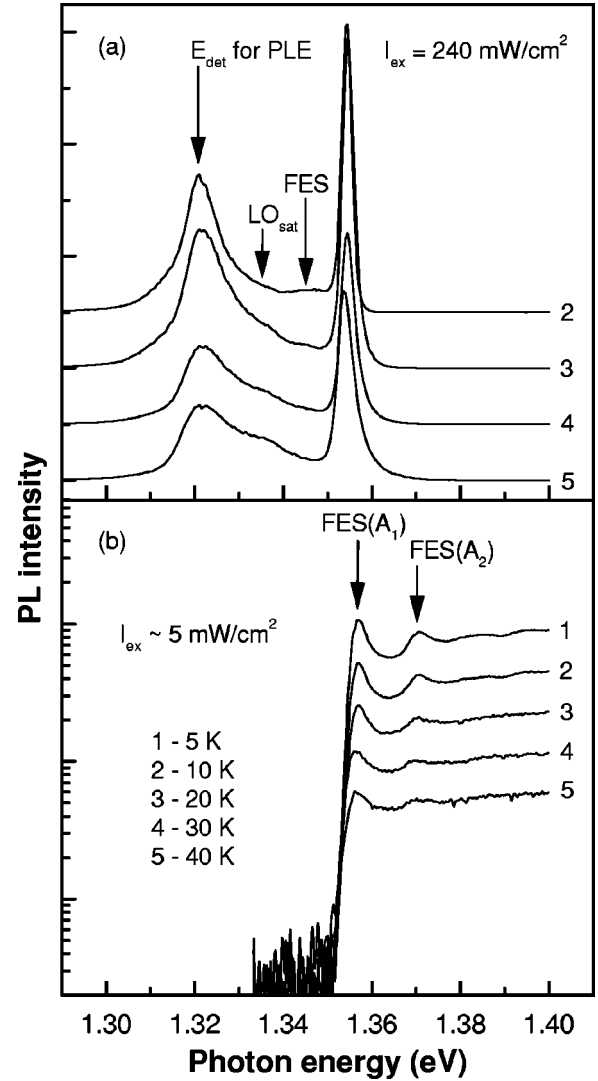


FIG. 5. Temperature-dependent development of the PL (a) and PLE (b) spectra of sample 1. The FES and its LO satellite are marked by arrows.

questionable. Indeed, the calculated electron-hole wave function overlaps exhibit no substantial variation within the investigated temperature range ($2 \text{ K} < T < 51 \text{ K}$), thus no reasonable explanations remain for the strong quenching of this peak at temperatures as high as 40 K.²⁷

In order to clarify the nature of feature B in the PL spectrum observed in our set of samples, the PLE spectra have been studied. Figure 5 depicts the PL (a) and PLE (b) spectra for sample 1 measured for various temperatures. PLE spectra do not reveal new electronic states below the E_2 state. Two pronounced peaks are, however, seen at the onset of absorption. These peaks demonstrate a strong temperature dependence and the high-energy peak completely decays at temperatures as high as 40 K. The PLE results correlate nicely with the temperature-dependent PL data. Figure 6 mirrors this correlation depicting the absorption (a) and recombination (b) scheme for optical transitions in case of two occupied electron subbands and the presence of localized holes. In absorption we find two vertical transitions (A_1 and A_2)

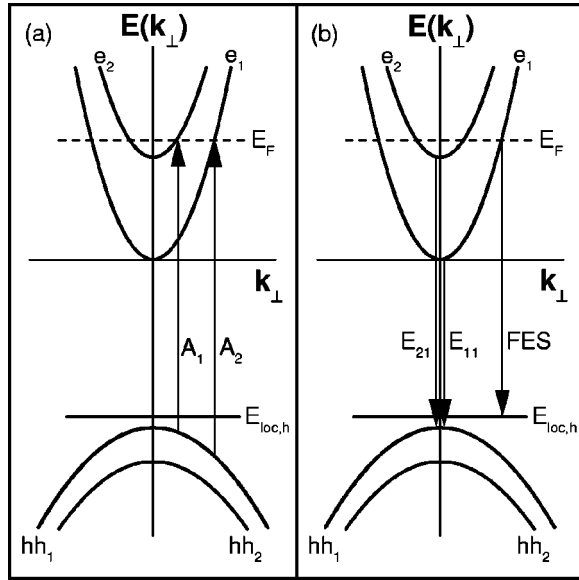


FIG. 6. Absorption (a) and recombination (b) scheme for optical transitions in case of two occupied electron subbands and the presence of localized holes.

from the heavy hole hh_1 state to the Fermi edge states at $k_{F,n}$ ($n=1,2$), that correspond to the k -vector value for Fermi energy in $n=1$ and $n=2$ electronic subbands, respectively. These transitions demonstrate the FES enhancement both for the $n=1$ (FES feature for transition A_2) and for the $n=2$ (FES feature for transition A_1) subbands in the PLE spectrum, respectively. The energy difference $E_{hh_1}(k_{F,1}) - E_{hh_1}(k_{F,2})$ calculated in the nonparabolic fourband approximation gives 12 meV being close to the energetic distance $F(A_2) - F(A_1) = 14$ meV measured in the PLE spectrum, where F denotes Fermi-edge singularity. Such a behavior is in agreement with theoretical predictions for the case in which the second electron subband is really populated by free carriers.¹² In this case two singularities should appear arising from the first and second Fermi wave vectors $k_{F,1}$ and $k_{F,2}$ in each electron subband. The main contribution to the spectrum in the ladder approximation will arise from the $G_{00;10} + G_{01;00}$ terms in the Bethe-Salpeter equations for interacting electron-hole Green's functions $G_{ij;kl}$.¹² In this case the off-diagonal term $G_{00;01}$ represents the mixing of $hh_1 - e_1$ and $hh_1 - e_2$ transitions, giving rise to the FES enhancement.

In the PL spectrum the corresponding FES features will arise at the E_{21} transition energy and at the energy, shifted toward lower energies by value of the localization energy for heavy holes, as follows from Fig. 6(b). This shift occurs to be 14 meV for the FES feature seen in the PL spectra of Fig. 5(a). In order to explain the FES dependences on temperature and excitation density observed both in sample 1 and sample 2 we propose, following Mueller *et al.*,²⁸ that the development of a strong enhancement of the oscillator strength for transitions at E_F in the E_1 subband is due to $E_1 \leftrightarrow E_2$ inter-subband Coulomb scattering of electrons. This possibility is recently discussed. As demonstrated experimentally, non-Coulomb scattering can efficiently control the

formation of FES in multi-subband heterostructures. The alloy dependent inter-subband scattering may easily prevail over multiple diffusions from charged valence holes expected by many-body processes. We account for the significant spectral shift (~ 15 meV) of the FES from the E_F position, which is not predicted in Ref. 28, as the localization energy for the heavy hole. The *ad hoc* addition allows at least qualitative agreement between the model prediction^{1,11} and the PL enhancement behavior.

The hole localization is of importance for several reasons. The conservation rules for optical processes cannot be fulfilled for electrons at the Fermi energy ($k_F \sim 2.5 \times 10^6$ cm⁻¹) if the free holes are relaxed into the states of the lowest energy at the top of the valence band with $k \approx 0$. Localized hole states may be viewed as being constructed from states with a range of momenta and therefore allow the PL from the vicinity of the Fermi level to be observed. The heavy holes can be localized by a form of disorder, typically alloy fluctuations in $\text{In}_y\text{Ga}_{1-y}\text{As}$ QW.²⁹ The origin of the hole localization in our samples has been explored in some detail by means of optical detection of quantum oscillations (ODQO) of the PL intensity in a magnetic field in Ref. 30. These data show that the quantum oscillations have two distinct periods in $1/B$. Such a behavior is directly addressed to the existence of two classes of hole localization: (i) a shallow one, primarily resulting in hole scattering, and (ii) a deeper localization resulting in a 10 ± 3 meV decrease of the free hole energy. A radius of the localized hole wave function is estimated to be of 10–30 Å, similar to what is deduced from the magnitude of the strong exciton-LO-phonon coupling typical for this QW.

The presence of strongly localized heavy holes allows their recombination with electrons from the vicinity of the Fermi edge. The PL enhancement is due to the mixing of the subband states by the photoexcited hole and due to virtual excitations of electron-hole pairs involving a higher subband. Therefore, if one takes into account that the optical transitions occur between localized holes and the 2DEG from the Fermi-edge vicinity, the abnormally large FES shift towards smaller energies is expected. Further, the FES shift observed is approximately 12–15 meV, an energy that correlates well with the hole localization energy deduced from the ODQO measurements, 10 ± 3 meV.

Our PL data also contradict the expectation that for the finite hole mass the FES in both PL and absorption will be smeared out over the effective energetic range of the occupied valence band $[(m_e/m_h)E_F]$, leading to the destruction of the FES for even moderate Fermi energies.⁹ The unusual and strong temperature and excitation density dependences can be also ascribed to the long thermalization time for the photoexcited holes, due to the absence of efficient energy loss mechanisms, such as LO-phonon scattering, at the last stage of hole relaxation, leading to an increase of the hot hole population.

As alluded to above, the spectral enhancement at the blue side of the E_{11} transition clearly seen in the PL spectrum of sample 1 is probably due to the GaAs-like LO-phonon participation in the scattering processes of the electrons in the Fermi sea. Such LO-phonon-assisted indirect transitions are

known to be important in the relaxation of hot electrons at high densities.²⁵ The hole localization energy does not play a role in this phonon-assisted transition, because the phonon is able to supply the momentum difference between the Fermi-sea electrons and the free holes. In our case, the excitonic enhancement of the FES also promotes the phonon satellite seen as the shoulder in Fig. 4(a) at high temperatures.

IV. CONCLUSIONS

We have observed fundamentally different behavior related to many-body effects in the PL of high-density two-dimensional electron gas. The main characteristics of these observations are: (i) the FES enhancement from E_F of $n=1$ electronic subband is observed under condition of the $n=2$ subband population, (ii) the heavy-hole localization en-

ergy is directly observed in the FES development, (iii) the many-body enhancement becomes initially *stronger* with *increasing* temperature, and (iv) the FES is a nonmonotonic function of the excitation density. We have, furthermore, described a theoretical framework to explain these effects. Nevertheless, the self-consistent analysis of the experimental data is a theoretical challenge for further ascertainment both of the hole localization influence on the development of many-body effects and of peculiarities of the dynamic response of 2DEG in the case of elevated temperature and excitation density.

ACKNOWLEDGMENT

This work was supported by a NATO Linkage Grant.

*Electronic address: kissel@fbh-berlin.de

[†]Present address: Department of Physics, University of Arkansas, Fayetteville, Arkansas 72701.

[‡]Permanent address: Institute of Semiconductor Physics, National Academy of Sciences, Prospect Nauki 41, 03028 Kiev, Ukraine.

¹M. S. Skolnick, J. M. Rorison, K. J. Nash, D. J. Mowbray, P. R. Tapster, S. J. Bass, and A. D. Pitt, Phys. Rev. Lett. **58**, 2130 (1987).

²C. Delalande, G. Bastard, J. Orgonasi, J. A. Brum, H. W. Liu, M. Voos, G. Weimann, and W. Schlapp, Phys. Rev. Lett. **59**, 2690 (1987).

³C. Colvard, N. Nouri, H. Lee, and D. Ackley, Phys. Rev. B **39**, 8033 (1989).

⁴H. Kalt, K. Leo, R. Cingolani, and K. Ploog, Phys. Rev. B **40**, 12 017 (1989).

⁵G. Mahan, *Many Particle Physics* (Plenum, New York, 1981).

⁶S. Schmitt-Rink, D. S. Chemla, and D. A. B. Miller, Adv. Phys. **38**, 89 (1989).

⁷W. Chen, M. Fritze, A. V. Nurmikko, D. Ackley, C. Colvard, and H. Lee, Phys. Rev. Lett. **64**, 2434 (1990).

⁸T. Uenoyama and L. J. Sham, Phys. Rev. B **39**, 11 044 (1989).

⁹A. E. Ruckenstein and S. Schmitt-Rink, Phys. Rev. B **35**, 7551 (1987).

¹⁰J. F. Mueller, Phys. Rev. B **42**, 11 189 (1990).

¹¹P. Hawrylak, Phys. Rev. B **44**, 3821 (1991).

¹²F. J. Rodriguez and C. Tejedor, J. Phys.: Condens. Matter **8**, 1713 (1996).

¹³G. Livescu, D. A. B. Miller, D. S. Chemla, M. Ramaswamy, T. Y. Chang, N. Sauer, A. C. Gossard, and J. H. English, IEEE J. Quantum Electron. **QE-24**, 1677 (1988).

¹⁴S. A. Brown, J. F. Young, J. A. Brum, P. Hawrylak, and Z. Wasilewski, Phys. Rev. B **54**, 11 082 (1996).

¹⁵S. A. Brown, J. F. Young, Z. Wasilewski, and P. T. Coleridge, Phys. Rev. B **56**, 3937 (1997).

¹⁶H. P. van der Meulen, I. Santa-Olalla, J. Rubio, J. M. Calleja, K. J. Friedland, R. Hey, and K. Ploog, Phys. Rev. B **60**, 4897 (1999).

¹⁷V. Huard, R. T. Cox, K. Saminadayar, A. Arnoult, and S. Tatarenko, Phys. Rev. Lett. **84**, 187 (2000).

¹⁸T. Mélin and F. Laruelle, Phys. Rev. Lett. **76**, 4219 (1996).

¹⁹T. Mélin and F. Laruelle, Phys. Rev. Lett. **85**, 852 (2000).

²⁰H. Kissel, U. Müller, C. Walther, W. T. Masselink, Yu. I. Mazur, G. G. Tarasov, G. Yu. Rud'ko, M. Ya. Valakh, V. Malyarchuk, and Z. Ya. Zhuchenko, Phys. Rev. B **61**, 8359 (2000).

²¹I. A. Buyanova, T. Lundström, A. V. Buyanov, W. M. Chen, W. G. Bi, and C. W. Tu, Phys. Rev. B **55**, 7052 (1997).

²²M. S. Skolnick, D. M. Whittaker, P. E. Simmonds, T. A. Fisher, M. K. Saker, J. M. Rorison, R. S. Smith, P. B. Kirby, and C. R. H. White, Phys. Rev. B **43**, 7354 (1991).

²³S. J. Xu, S. J. Chua, X. H. Tang, and X. H. Zhang, Phys. Rev. B **54**, 17 701 (1996).

²⁴W. T. Masselink, H. Kissel, U. Müller, C. Walther, Yu. I. Mazur, G. G. Tarasov, G. Yu. Rud'ko, M. Ya. Valakh, V. Malyarchuk, and Z. Ya. Zhuchenko, Semicond. Phys. Quantum Electron. Optoelectron. **3**, 126 (2000).

²⁵W. Chen, M. Fritze, W. Walecki, A. V. Nurmikko, D. Ackley, J. M. Hong, and L. L. Chang, Phys. Rev. B **45**, 8464 (1992).

²⁶U. Fano, Phys. Rev. **124**, 1866 (1961).

²⁷M. L. F. Abbade, F. Iikawa, J. A. Brum, Th. Tröster, A. A. Bernussi, R. G. Pereira, and G. Borghs, J. Appl. Phys. **80**, 1925 (1996).

²⁸J. F. Mueller, A. E. Ruckenstein, and S. Schmitt-Rink (unpublished). For reference see Ref. 20.

²⁹L. V. Butov, V. D. Kulakovskii, T. G. Andersson, and Z. G. Chen, Phys. Rev. B **42**, 9472 (1990).

³⁰G. G. Tarasov, U. Müller, Yu. I. Mazur, H. Kissel, Z. Ya. Zhuchenko, C. Walther, and W. T. Masselink, Phys. Rev. B **58**, 4733 (1998).